Supplementary Information

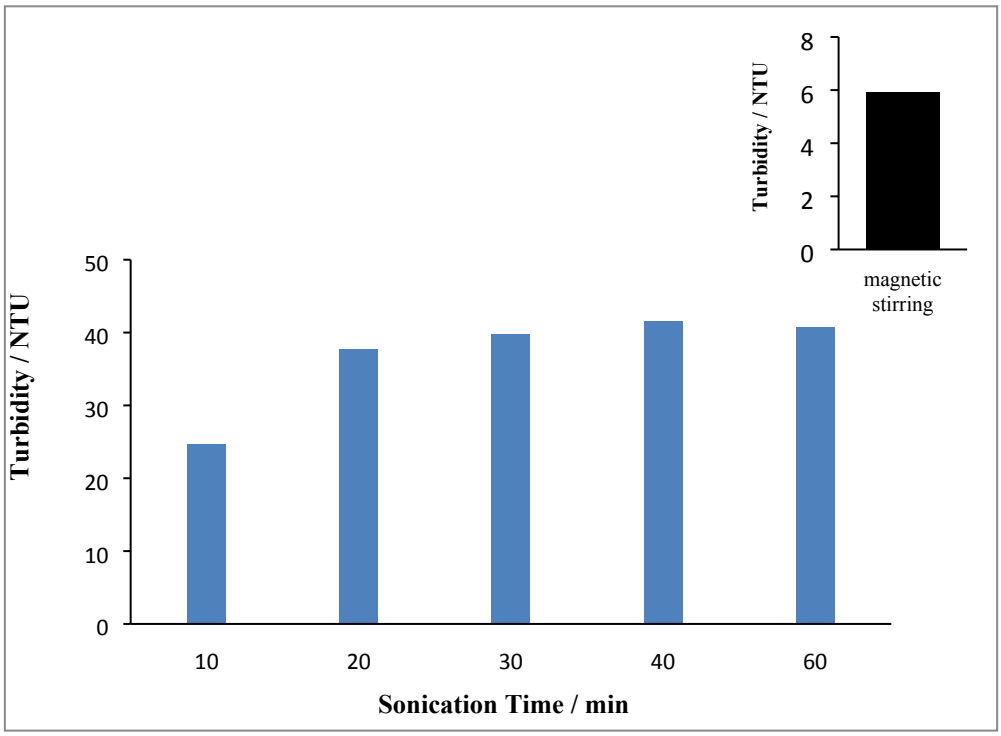

Figure S1. Plots of turbidity of dispersion ZnO in the aqueous phase versus sonication time, inset figure shows: turbidity after 40 min magnetic stirring.

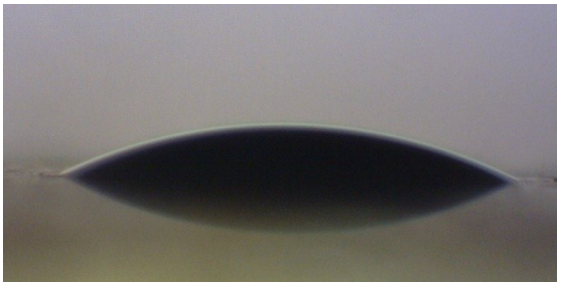

Figure S2. The images of water drop on the surface of ZnO nanoparticles thin film.

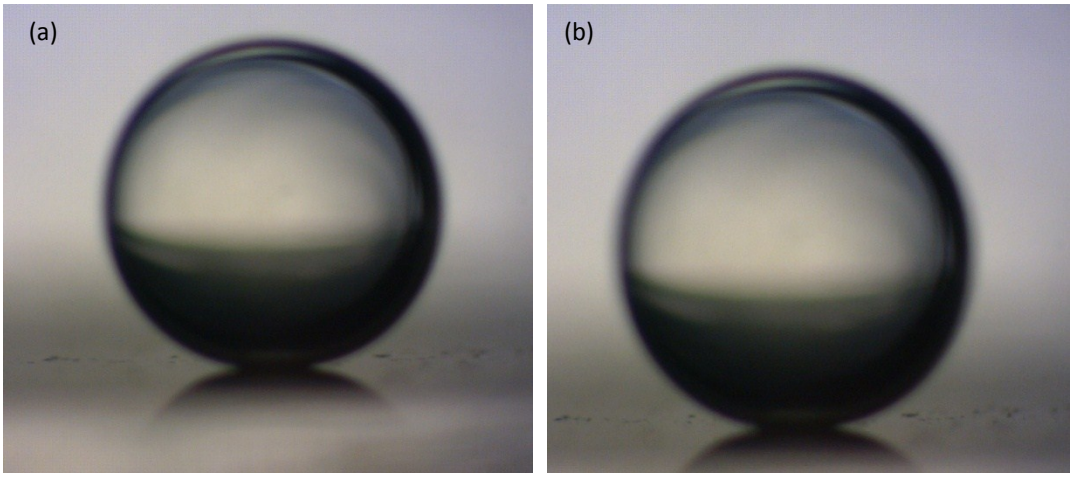

Figure S3. The images of water drop covered by n-decane at a quartz substrate in the absence (a) and presence of ZnO nanoparticles.

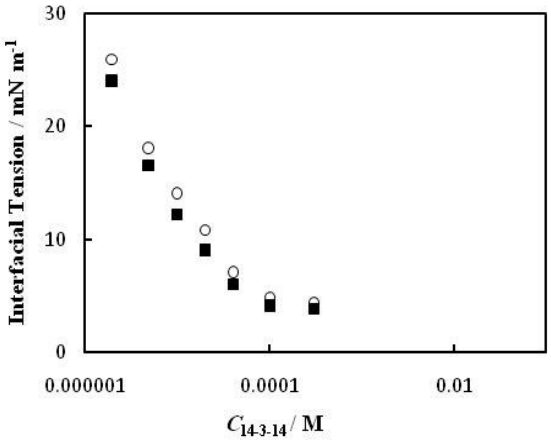

Figure. S4 The equilibrium interfacial tension of aqueous 14-3-14 solution /n-decane vs. surfactant concentration in the absence ○, and presence ■ of 0.01 wt% ZnO nanoparticles at 25 °C.

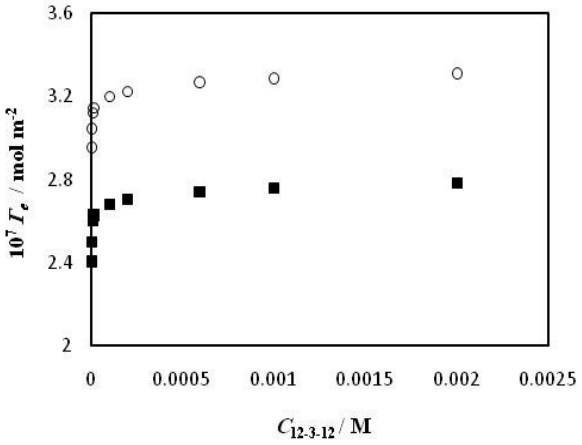

Figure S5. Equilibrium surface concentration vs. 12-3-12 bulk concentration in the absence ○ and presence ■ of 0.01 wt% ZnO nanoparticles at 25 °C.

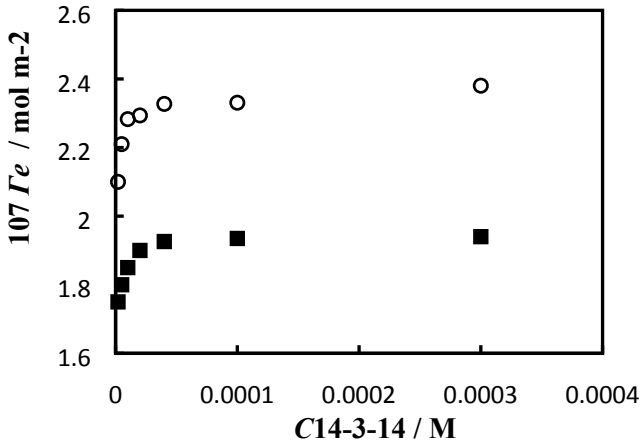

Figure S6. Equilibrium surface concentration vs. 14-3-14 bulk concentration in the absence ○ and presence ■ of 0.01 wt% ZnO nanoparticles at 25 °C.

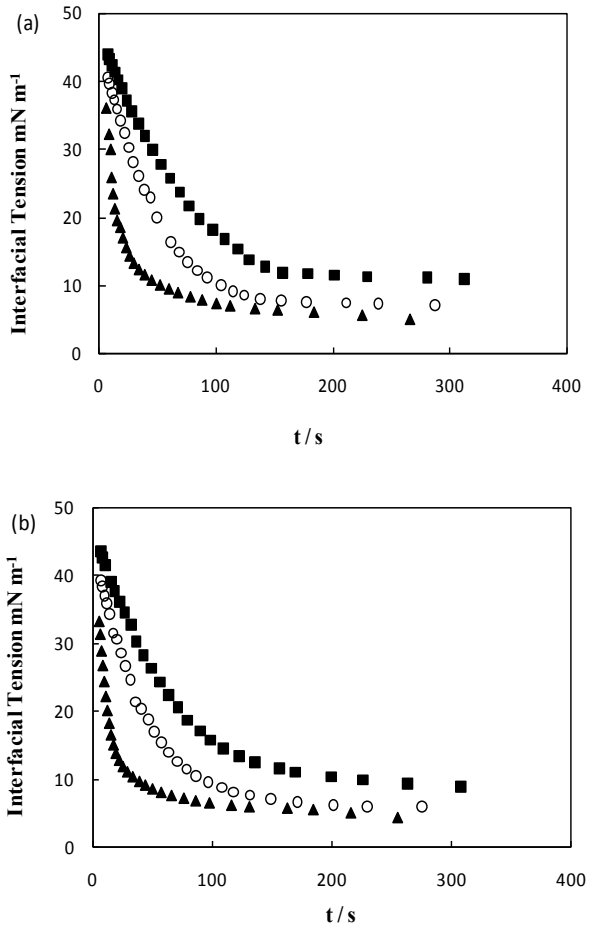

Figure S7. The dynamic interfacial tension of 14-3-14 aqueous solution / n-decane vs. time at 25 °C and at different SDS concentrations; 0.00002 ■, 0.00004 ○, 0.0001▲, M. (a) in the absence and (b) in the presence of 0.01 wt% ZnO nanoparticles.

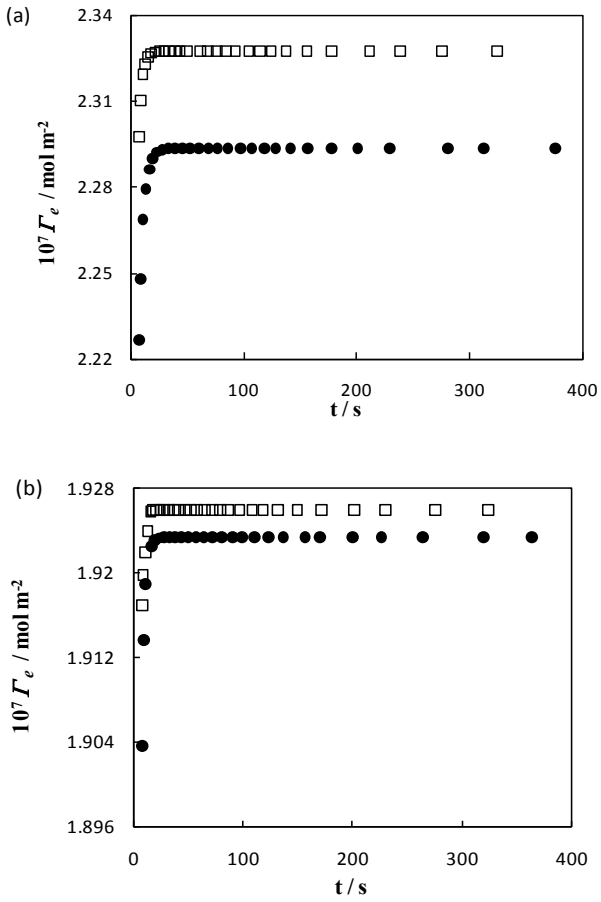

Figure S8. Dynamic surface concentration vs. time at different 14-3-14 concentrations, 0.000006 □ and 0.00004 ● M. (a) in the absence and (b) in the presence of 0.01 wt% ZnO nanoparticles at 25 °C.

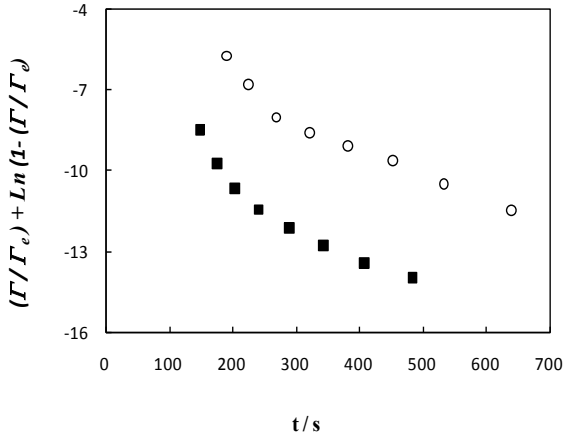

Figure S9. The plot of $\frac{\Gamma}{\Gamma_e} + \ln\left(1 - \frac{\Gamma}{\Gamma_e}\right)$ vs. time close to equilibrium for 0.00001 M 12-3-12 concentration, in the absence ○ and in the presence ■ of 0.01 wt% ZnO nanoparticles at 25 °C.

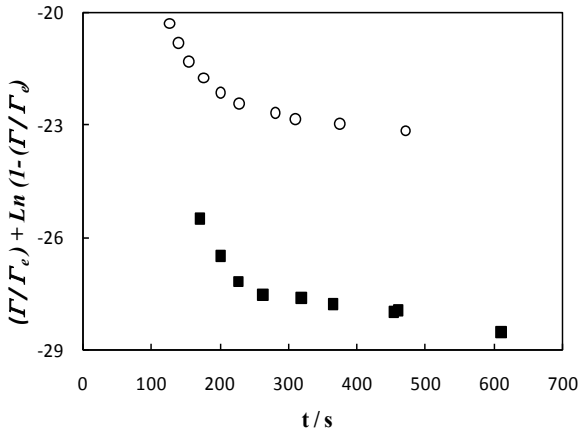

Figure S10. The plot of $\frac{\Gamma}{\Gamma_e} + \ln\left(1 - \frac{\Gamma}{\Gamma_e}\right)$ vs. time close to equilibrium for 0.00002 M 14-3-14 concentration, in the absence ○ and in the presence ■ of 0.01 wt% ZnO nanoparticles at 25 °C.

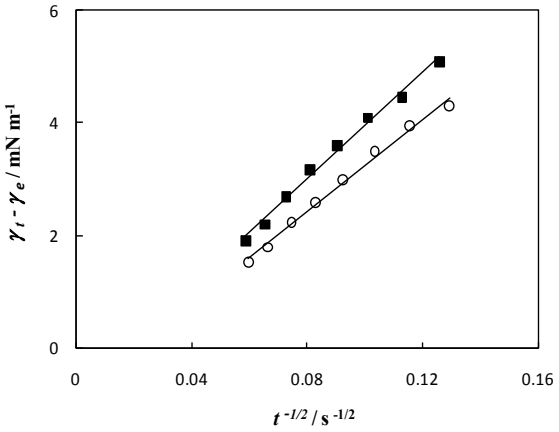

Figure S11. Plot of $\gamma(t)_{t\to\infty} - \gamma_e$ vs. $t^{-1/2}$ for close to equilibrium data at 0.000004, M of 14-3-14, in the absence ○ and presence ■ of 0.01 wt% ZnO nanoparticles at 25 °C.

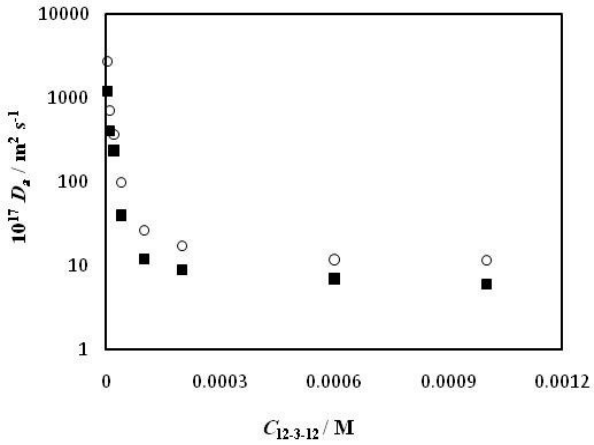

Figure S12. Apparent diffusion coefficient D_a as a function of 12-3-12 bulk concentration in the absence ○ and presence ■ of ZnO nanoparticles at 25 °C.

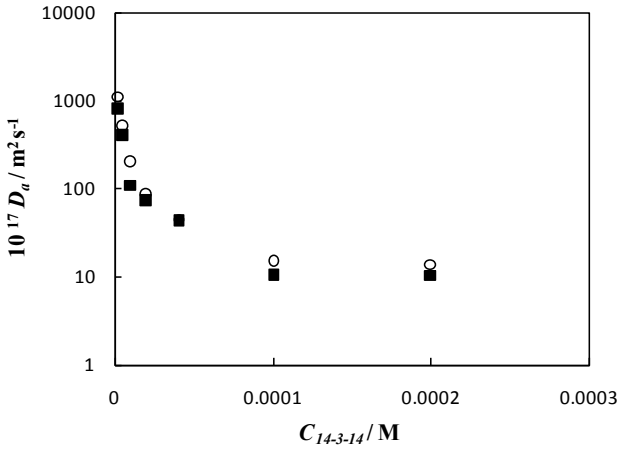

Figure S13. Apparent diffusion coefficient D_a as a function of 14-3-14 bulk concentration in the absence ○ and presence ■ of ZnO nanoparticles at 25 °C.

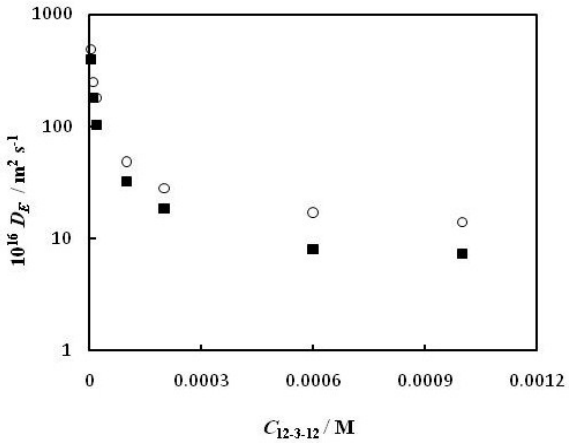

Figure S14. Effective diffusion coefficient D_E as a function of 12-3-12 bulk concentration in the absence ○ and presence ■ of ZnO nanoparticles at 25 °C.

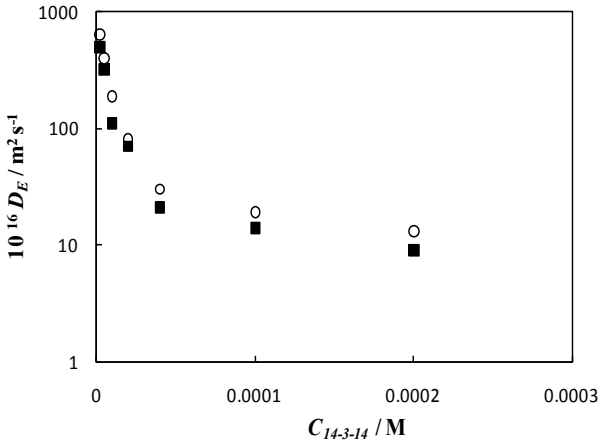

Figure S15. Effective diffusion coefficient D_E as a function of 14-3-14 bulk concentration in the absence ○ and presence ■ of ZnO nanoparticles at 25 °C.

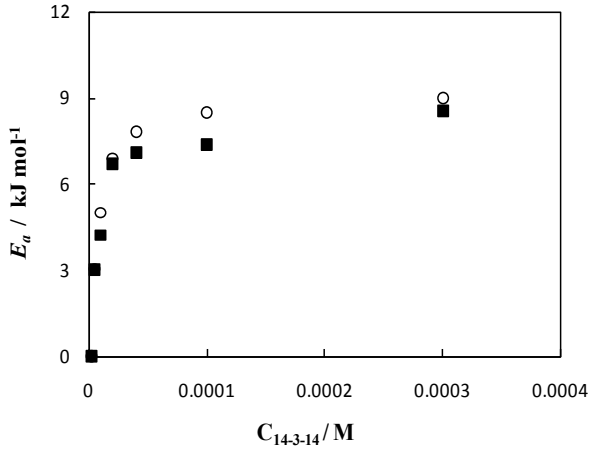

Figure S16. Activation energy of adsorption, E_a, as a function of 14-3-14 bulk concentration in the in the absence ○ and presence ■ of ZnO nanoparticles at 25 °C.

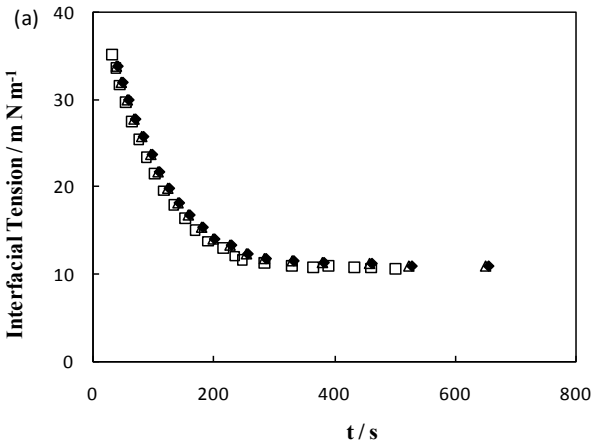

Figure S17. Effect of solution pH on the dynamic interfacial tension for $C_{14\text{-}3\text{-}14}$=0.000015 M, pH=5.5 Δ, pH=7○and pH=9.5 ♦ (a) in the absence and (b) in the presence of 0.01 wt% ZnO nanoparticles at 25 °C.

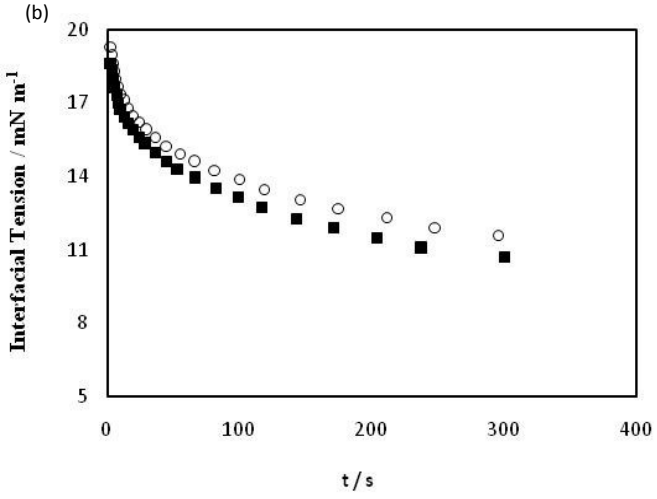

Figure S18. Dynamic interfacial tension of 12-3-12 surfactant aqueous solution / n-decane vs. time in the 0.005○ and 0.01 ■ wt% of ZnO nanoparticles at 25 °C.

(a)

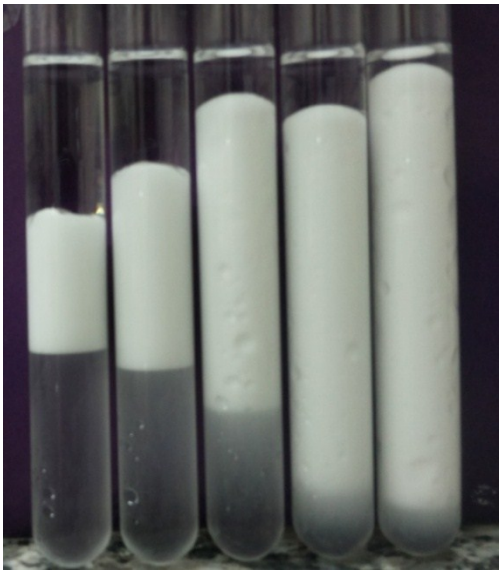

(b)

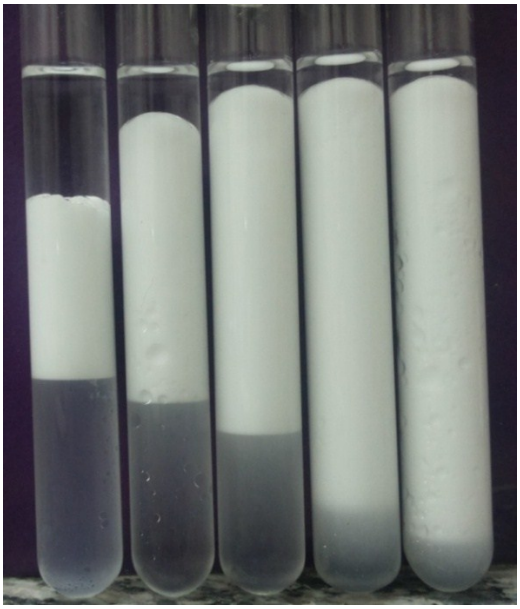

Figure S19. Photograph of vessels containing emulsions of decane and water (1:1) stabilized by (a) 14-3-14 surfactant alone at concentrations of 0.00001, 0.00004, 0.00008, 0.0001 and 0.0002 M (left to right). (b) A fixed concentration of ZnO nanoparticles (0.01 wt %) and 12-3-12 with the same concentrations of (a).

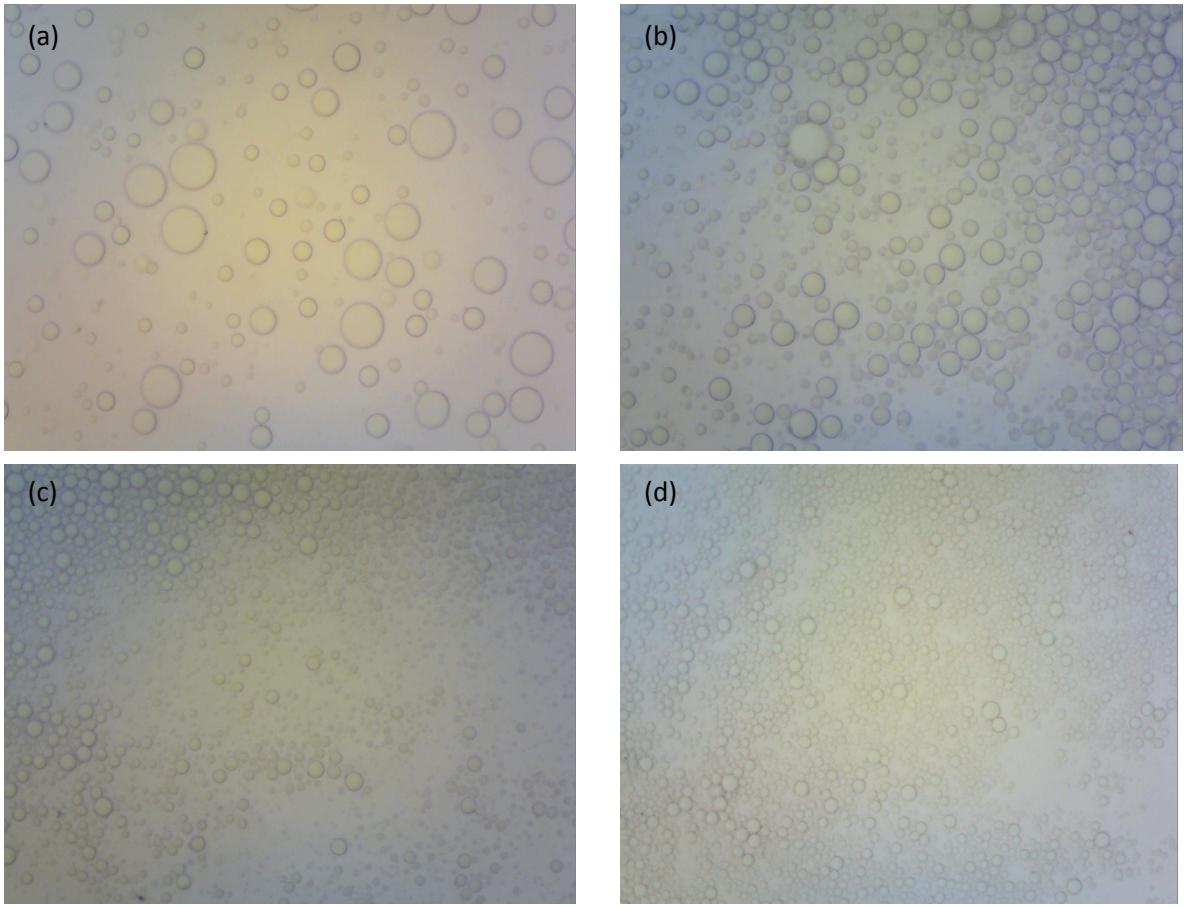

Figure S20. Optical microscopy image of n-decane-in-water emulsions (1:1) stabilized by (a) 0.00001 M 14-3-14 alone, and mixture of 0.01 wt % ZnO particles, and (b) 0.00001, (c) 0.0001, and (d) 0.001 M 14-3-14. With × 400 magnification.